Atmospheric Environment 129 (2016) 142–154

Contents lists available at ScienceDirect

Atmospheric Environment

journal homepage: www.elsevier.com/locate/atmosenv

Water uptake by organic aerosol and its influence on gas/particle partitioning of secondary organic aerosol in the United States

Shantanu H. Jathar [a], Abdullah Mahmud [b], Kelley C. Barsanti [b], William E. Asher [c], James F. Pankow [b, d], Michael J. Kleeman [a, *]

[a] Civil and Environmental Engineering, University of California, Davis, CA, USA
[b] Civil and Environmental Engineering, Portland State University, Portland, OR, USA
[c] Applied Physics Laboratory, University of Washington, Seattle, WA, USA
[d] Chemistry, Portland State University, Portland, OR, USA

HIGHLIGHTS

- Organic-phase water is predicted in eastern US and California using the same model.
- Organic-phase water enhances SOA formation in the eastern US.
- Organic-phase water has small effect on SOA formation in California.
- Different behavior is driven by regional emissions profiles.
- Particle mixing state changes the impact of organic-phase water.

ARTICLE INFO

Article history:
Received 20 January 2015
Received in revised form
28 August 2015
Accepted 4 January 2016
Available online 7 January 2016

Keywords:
Organic-phase water
Secondary organic aerosol
California
Eastern United States
Source-oriented external mixture

ABSTRACT

Organic aerosol (OA) is at least partly hygroscopic, i.e., water partitions into the organic phase to a degree determined by the relative humidity (RH), the organic chemical composition, and the particle size. This organic-phase water increases the aerosol mass and provides a larger absorbing matrix while decreasing its mean molecular weight, which can encourage additional condensation of semi-volatile organic compounds. Most regional and global atmospheric models account for water uptake by inorganic salts but do not explicitly account for organic-phase water and its subsequent impact on gas/particle partitioning of semi-volatile OA. In this work, we incorporated the organic-phase water model described by Pankow et al. (2015) into the UCD/CIT air quality model to simulate water uptake by OA and assessed its influence on total OA mass concentrations. The model was run for one summer month over two distinct regions: South Coast Air Basin (SoCAB) surrounding Los Angeles, California and the eastern United States (US). In SoCAB where the OA was dominated by non-hygroscopic primary OA (POA), there was very little organic-phase water uptake (0.1–0.2 μg m^{-3}) and consequently very little enhancement (or growth) in total OA concentrations (OA + organic-phase water): a 3% increase in total OA mass was predicted for a 0.1 increase in relative humidity. In contrast, in the eastern US where secondary OA (SOA) from biogenic sources dominated the OA, substantial organic-phase water uptake and enhancement in total OA concentrations was predicted, even in urban locations. On average, the model predicted a 20% growth in total OA mass for a 0.1 increase in relative humidity; the growth was equivalent to a 250 nm particle with a hygroscopicity parameter (κ) of 0.15. Further, for the same relative humidity, the exact extent of organic-phase water uptake and total OA enhancement was found to be dependent on the particle mixing state. When the source-oriented mixing state of aerosols was considered, generally, less organic-phase water uptake was predicted than when simple internal mixing approximations were made. Overall, the results indicated that organic-phase water can significantly influence predicted total OA concentrations under certain conditions. Regional models applied in areas with high humidity and significant SOA formation should include calculations for organic-phase water in order to capture this effect.

* Corresponding author.
E-mail address: mjkleeman@ucdavis.edu (M.J. Kleeman).

http://dx.doi.org/10.1016/j.atmosenv.2016.01.001
1352-2310/

1. Introduction

Organic aerosol (OA) accounts for a third of the ambient submicron aerosol mass (Jimenez et al., 2009) globally with significant implications for the energy budget of the earth (Pachauri et al., 2014) and human health (IHME, 2013). Despite its abundance, OA is one of the least understood components of atmospheric aerosol (Hallquist et al., 2009).

Although less hygroscopic than inorganic salts like sodium chloride and ammonium sulfate, laboratory-generated and ambient OA has been shown to be hygroscopic, i.e. depending on the particle size, the OA composition and the ambient relative humidity (RH) OA, will absorb water.[1] This organic-phase water (defined to be water in the organic phase) can alter the thermodynamic, reactive and optical behavior of OA and in turn affect the climate and health–relevant properties of OA (Kanakidou et al., 2005). OA is a complex mixture of thousands of different compounds (Goldstein and Galbally, 2007) that arise from numerous sources and reaction pathways, each with a different set of physical and chemical properties. Hence, individual constituents of OA exhibit varying levels of hygroscopicity when present as pure compounds. The hygroscopicity parameter (κ) is a measure of the ability of a molecule/mixture to absorb water; inorganic acids and salts like sodium chloride and ammonium sulfate have κ values larger than 0.6 (Koehler et al., 2009). Small acids found in ambient OA like malonic and glutaric acid or oxygenated organic compounds found in biomass burning emissions like levoglucosan are modestly hygroscopic, with pure-compound κ values of 0.44, 0.2 and 0.165 respectively (Koehler et al., 2009). In contrast, κ values less than 0.01 have been measured for primary organic aerosol (POA) from diesel exhaust (Weingartner et al., 1997). Further, constituents of OA constantly evolve in the atmosphere (e.g., via photochemical aging), changing their hygroscopic properties. For example, Jimenez et al. (2009) showed that the hygroscopicity of secondary organic aerosol (SOA) formed from the gas-phase oxidation of aromatic and biogenic volatile organic compounds (VOC) increased as the SOA become increasingly oxidized. Overall, it is expected that ambient OA will display a wide range of water uptake characteristics that will change as the chemical composition of OA evolves.

Petters and Kreidenweis (2007) used surrogate organic molecules to demonstrate that the effective hygroscopicity of OA can be estimated using a mixing rule that weights constituent hygroscopicities by their volume fractions in the OA mixture. This mixing rule provides a simple representation to model the hygroscopicity or water uptake (and cloud condensation nuclei activity) of OA (and other aerosols) in large-scale models (Liu and Wang, 2010; Pringle et al., 2010). However, the mixing rule assumes that the constituents of OA and water do not interact with each other at a molecular level (i.e., thermodynamically). Over the past decade, several studies have used activity coefficient models like UNIFAC (UNIquac Functional-group Activity Coefficient; Fredenslund et al. (1975)) to model water uptake based on the molecular interaction of aerosol constituents and water (Ansari and Pandis, 2000; Clegg et al., 2001; Seinfeld et al., 2001; Peng et al., 2001; Ming and Russell, 2002; Bowman and Karamalegos, 2002; Griffin et al., 2005; Barley et al., 2009; Zuend et al., 2010; Zuend and Seinfeld, 2012). Most found that water uptake by the OA fraction was limited compared to that by the inorganic fraction. However, the water uptake was sufficient to modify the activity of the SOA species and the mass and mean molecular weight of the absorbing organic phase. This altered the gas/particle partitioning and enhanced SOA mass concentrations by 10–100% at an RH of 80% for a wide range of precursor/oxidant systems (Seinfeld et al., 2001; Barley et al., 2009). At lower OA mass concentrations, Pankow and Chang (2008) found that the SOA enhancements were as high as a factor of 5 and an RH of 80% for the α-pinene/O_3 and isoprene/OH system.

Most large-scale models, supported by ambient observations of a well-mixed aerosol, assume that SOA is "miscible" with POA and can absorptively partition into POA. However, laboratory studies probing the miscibility of POA and SOA are equivocal. It has been suggested that fresh emissions of POA from diesel exhaust (Asa-Awuku et al., 2009) and biomass burning (Kanakidou et al., 2005) can mix with SOA while model compounds/surrogates for POA like dioctyl phthalate, adipic and fulvic acid, diesel fuel and lubricating oil do not (Asa-Awuku et al., 2009; Song et al., 2007, 2011). The miscibility of POA and SOA will determine not only the total uptake of water but will also modify the influence water has on the gas/particle partitioning of OA. For an activity coefficient model like UNIFAC, the modeled molecular interactions within an OA and water system will, hence, be sensitive to assumptions made about the miscibility of POA and SOA and contribute to uncertainty in model predictions of OA and organic-phase water. Further, almost all large-scale models assume that ambient aerosol is internally mixed, which might not always be a good assumption for urban aerosol (Schwarz et al., 2008) where differences in OA composition across particle types will lead to varying water uptake and subsequent effects on gas/particle partitioning of OA. Model predictions of OA and organic-phase water will, hence, be sensitive to assumptions about the mixing state of aerosol. These assumptions about POA-SOA miscibility and the aerosol mixing state add uncertainty to model predictions of OA and organic-phase water and, in the context of the current work (i.e., role of water on OA), have not previously been explored in large-scale models.

Examples of the explicit treatment of water uptake by OA and its influence on gas/particle partitioning of semi-volatile OA in a chemical transport or a climate model are limited mostly because of the computational expense of running an activity coefficient model in a three-dimensional framework. In fact, we are only aware of two studies that used activity coefficient models to predict the effects of organic-phase water. The first is by Pun (2008) where a single day was simulated in the eastern United States (US) for the summer of 2002. This work used a simpler model (Wilson equation) to calculate activity coefficients for the OA-organic-phase water mixture and did not represent important processes such as "oligomerization" (aka accretion reactions). The second is the work by Pankow et al. (2015) – a companion paper to this work – that simulates the influence of organic-phase water on SOA partitioning over a 10-day episode in the eastern US. We build on the latter study to explore the sensitivity of water uptake by OA and subsequent SOA gas/particle partitioning in different geographical domains (South Coast Air Basin (SoCAB) versus eastern US) to assumptions about the miscibility of POA and SOA and the mixing state of the aerosol (internally versus source-oriented externally mixed aerosol).

2. Methods

2.1. Chemical transport model

We used the UCD/CIT (University of California/California Institute of Technology) air quality model to simulate organic-phase water uptake and its influence on the gas/particle partitioning of OA. The UCD/CIT model is a regional chemical transport model

[1] In this manuscript, the word "organic-phase water" is exclusively used to refer to the water associated with the organic fraction of ambient aerosol. This "organic-phase water" is separate from the water associated with the inorganic fraction of ambient aerosol.

(CTM) that simulates the emissions, transport, gas-phase chemistry, aerosol physics and chemistry (dynamic gas/particle partitioning, coagulation and thermodynamics and deposition) in the troposphere. Modules used to represent various processes in the model are described elsewhere: transport (Kleeman and Cass, 2001; Hu et al., 2010), gas-phase chemical mechanism (Carter and Heo, 2013), inorganic aerosol thermodynamics (Nenes et al., 1998) and deposition (Kleeman et al., 1997; Mahmud et al., 2010). Here, we only describe updates made to the UCD/CIT model. Table 1 lists key features of and inputs for the UCD/CIT model.

We employed the condensed form of the SAPRC-11 gas-phase chemical mechanism; the SAPRC-11 mechanism differs from the SAPRC-07 version used in earlier versions of the UCD/CIT model (Hu et al., 2012) in that it has an improved treatment of chemistry of aromatic VOCs. The uptake of N_2O_5 to the aqueous phase was parameterized using the work of Davis et al. (2008). The UCD/CIT model relied on offline meteorology to simulate tropospheric processes that affect predicted air quality. Hourly meteorological fields were generated using the Weather Research and Forecasting (WRF) v3.4 model (www.wrf-model.org). North American Mesoscale (NAM) analysis data from the National Center for Environmental Protection were used to set the initial and boundary conditions for WRF. Following Baker et al. (2013), WRF was run for SoCAB using the asymmetric convective model planetary boundary layer scheme, Pleim-Xiu land surface model, and grid and surface nudging. For the eastern US, WRF was run using the Yonsei University scheme, Noah land surface model, and no nudging (LeMone et al., 2010b,a).

Anthropogenic emissions for California for 2005 were based on the inventory developed for the California Regional PM10/PM2.5 Air Quality Study (CRPAQS) of 2000. Mobile source emissions were calculated for 2005 by scaling emissions in 2000 by fuel consumption activity (CARB, 2011); emissions for area sources, point sources, and off-road sources were not changed from their year 2000 levels. Wildfire emissions were based on the Fire Inventory from National Center for Atmospheric Research (FINN, NCAR) (Wiedinmyer et al., 2011). Biogenic emissions were calculated using the Model of Emissions of Gases and Aerosols from Nature (MEGAN) (Guenther et al., 2006). All emissions were gridded using the University of California, Davis (UCD) emissions processor. In the eastern US, anthropogenic and wildfire emissions for the year 2006 were based on the 2005 National Emissions Inventory and gridded using the Sparse Matrix Operator Kernel Emissions (SMOKE) model version 2.5. Biogenic emissions were calculated using the Biogenic Emissions Inventory System version 3 (BEIS) and gridded using SMOKE version 2.5. Gas- and particle-phase initial and boundary conditions were obtained from MOZART-4/NCEP; more details can be found in Emmons et al. (2010) and at the website: http://www.acd.ucar.edu/wrf-chem/mozart.shtml. Boundary conditions varied with time and were updated hourly in the present study.

The UCD/CIT model was used to simulate air quality in two geographically-distinct domains: (1) the state of California at a grid resolution of 24 km × 24 km followed by a nested simulation over SoCAB at a grid resolution of 8 km × 8 km; and (2) the eastern half of the US, roughly east of the great continental divide at a grid resolution of 36 km × 36 km. The UCD/CIT model was run for California from July 15th to August 2nd, 2005 and for the eastern US from August 15th to September 2nd, 2006.

In all simulations described below, POA was assumed to be non-volatile as per the treatment in the Community Multiscale Air Quality (CMAQ) model version 4.7. The results in the current study will show that the non-volatile POA simplification has relatively minor consequences in the Eastern US where OA is dominated by biogenic SOA. The non-volatile POA simplification has greater potential consequences in California where POA dominates total OA. PM emissions factors and source profiles used in the California simulations were measured under atmospherically relevant conditions, meaning that emitted PM was diluted with clean air to concentrations that are close to those found in the real atmosphere. In some cases, this realistic dilution factor was intentionally chosen by selecting large amounts of dilution air, while in other cases it resulted from dramatic reductions in recent emissions rates while using a constant amount of dilution air. In either case, these realistic dilution factors largely mitigate the evaporation and re-condensation of POA that occurs when source profiles are measured at unrealistically high concentrations.

2.2. Base OA model

The SAPRC-11 model species ALK5 (representing C_7 and larger alkanes), BENZ (benzene), ARO1/ARO2 (aromatics except benzene), ISOP (isoprene), TERP (monoterpenes) and SQT (sesquiterpenes) were modeled to form SOA as per the formation pathways in CMAQ version 4.7 (Carlton et al., 2010). This included the gas-phase oxidation of the above-mentioned precursors to form semi-volatile products that partition into the particle-phase (using the two-product approach), the acid enhancement of isoprene SOA and particle-phase oligomerization. Here, POA and SOA were allowed to mix and form a single phase. Fully dynamic gas/particle partitioning was modeled as in the work of Kleeman and Cass (2001). Briefly, a 15-bin moving sectional model is used to capture the particle size distribution where the aerosol general dynamic equation is solved over each size bin to account for condensation/evaporation and coagulation; nucleation is not considered. The UCD/CIT model does not simulate cloud chemistry at this time and hence we did not include cloud and fog-driven production of SOA.

Table 1
Details of the chemical transport model and modeling system used in this work.

Domain	California	Eastern US
Resolution	24 km, nested 8 km	36 km
Grid cells	44 × 43; 63 × 30	65 × 65
Time period(s)	July 15 – Aug 13, 2005	Aug 15 – Sep 13, 2006
Meteorology	WRF v3.4 run with NAM reanalysis data	
Emissions	Anthropogenics: CARB (2011) Wildfires: NCAR Biogenics: MEGAN Gridded using UCD emissions processor	Anthropogenics + Wildfires: NEI (2005) Biogenics: MEGAN Gridded using SMOKE version 2.5
Gas-phase mechanism	SAPRC-11 (Carter and Heo, 2013)	
Inorganics	ISORROPIA (Nenes et al., 1998)	
Initial/boundary conditions	MOZART-4/NCEP (Emmons et al., 2010)	
SOA model	2-product model, acid-catalyzed SOA from isoprene, oligomerization, (Carlton et al., 2010)	

2.3. Water uptake and OA

We explicitly modeled the interaction of OA and organic-phase water using the UNIFAC model of Fredenslund et al. (1975). UNIFAC calculates the mole fraction-based activity coefficient (ζ_i) for each interacting molecule using a group contribution approach. POA and the SOA model species (both semi-volatile and non-volatile) were assigned groups based on the work of Chang and Pankow (2010) and described in detail in Pankow et al. (2015); for reference the groups are reproduced in Table S.1 in the supporting information. Briefly, the groups were determined using an iterative scheme in which the vapor pressure (calculated using the group contribution method SIMPOL (Pankow and Asher, 2008)) and molecular weight of the semi-volatile products were consistent with the two-product parameters in Carlton et al. (2010). Methods other than SIMPOL exist for predicting vapor pressure. However, as a group contribution method, SIMPOL (Pankow and Asher, 2008) is particularly well suited to our task of taking the assigned volatility in CMAQ and estimating consistent molecular structures. And, since we are not doing the reverse to predict vapor pressures, the use of SIMPOL does not affect the inherent volatility of the condensing molecules.

Once ζ_i for each model species was calculated by UNIFAC, the water activity was used along with the ambient RH to determine the partitioning of water into the organic phase. The organic-phase water increased the total absorbing mass (OA + organic-phase water) while lowering its mean molecular weight since the molecular weight of water (18 g mol^{-1}) is substantially lower than any of the SOA model species. Next, the ζi values were used to recalculate the gas/particle partitioning coefficient $K_{p,i}$ (m^3 μg^{-1}) (Pankow, 1994) by Eq. (1) where R is the ideal gas constant (8.206×10^{-5} m^3 atm mol^{-1} K^{-1}), T is the temperature in Kelvin, MW_{OA} is the mean molecular weight of the OA phase and $p^{\circ}_{L,i}$ is the pure compound vapor pressure of compound i as a liquid at temperature T.

$$K_{p,i} = \frac{760RT}{10^6 MW_{OA}\zeta_i p^{\circ}_{L,i}} \quad (1)$$

The updated $K_{p,i}$ values were used to calculate the gas/particle partitioning of the semi-volatile SOA species. The re-partitioning of the semi-volatile SOA species and organic-phase water changed the OA composition and hence the above steps were repeated until the system converged.

The OA model was run in four configurations (Table 2). In the first configuration, "Base", we did not model water uptake by OA and assumed that the POA mixed with SOA. The Base case served as the reference simulation to examine the effect of water uptake on OA levels. There is some laboratory evidence to suggest that POA surrogates might not be miscible with SOA (Asa-Awuku et al., 2009; Song et al., 2007). Hence in the second configuration, hereafter referred to as "Non-polar POA", we allowed for the uptake of water into SOA but we modeled POA as a large hydrocarbon (C_{25} n-alkane) that did not mix with the SOA + water phase. In essence, the OA phase was divided into two phases, a POA phase and an SOA + water phase. While fossil sources of POA might be hydrophobic enough to be immiscible with SOA, less hydrophobic (or more hydrophilic) POA from non-fossil sources such as meat cooking and biomass burning (Kanakidou et al., 2005), on account of their higher oxygen content, could potentially be miscible with SOA. Thus, to offer a representation of POA and SOA miscibility, in the third configuration hereafter referred to as "Chemically-resolved POA (internal)", we modeled POA from mobile sources as a large hydrocarbon (C_{25} n-alkane), POA from wood smoke and wildfires as levoglucosan, POA from food cooking as a generic monoglyceride and POA from all other sources as an n-octadecanoic acid. In this configuration, we allowed the uptake of water into SOA and polar POA (wood smoke, wildfires, food cooking, other sources) and kept the POA from mobile sources as a separate phase that did not mix with the SOA + polar POA + water phase. In all the configurations mentioned above, we considered OA to be internally mixed. Since the mixing state of the aerosol could affect model predictions, in the final configuration hereafter referred to as "Chemically-resolved POA (source-oriented)", we made the same assumptions about POA as in the Chemically-resolved POA (internal) configuration but we considered OA to be a source-oriented mixture using ten source types (on- and off-road gasoline and diesel, biomass, food cooking, coal, biogenics, other, boundary). POA + SOA from each source was tracked separately in the atmosphere without combining them into an internal mixture except through the relatively slow action of coagulation.

In this work, we explicitly assumed that the organic and inorganic aerosol, and the water associated with each, were phase separated based on the following arguments. First, almost all large-scale models assume a phase-separated organic and inorganic aerosol (we do not know of any regional or global model that simulates the thermodynamics of an organic, inorganic and water mixture together in an integrated model), although laboratory and ambient measurements find that ambient aerosol particles may have a single phase in special circumstances. Further, various experimental results (Bertram et al., 2011; Smith et al., 2013; Yatavelli et al., 2012; You et al., 2013, 2014) using model systems suggest that the phase separation in an organic + inorganic aerosol system is a strong function of the OA oxygen-to-carbon (O:C) ratio and a weak function of the inorganic composition and the organic to inorganic ratio. They show that phase separation is likely when O:C < 0.5 for the organic fraction, but unlikely when O:C > 0.7. Model predictions of OA in this work (and in most large-scale models (Tsigaridis et al., 2014)) are dominated by emissions of fresh POA and first-generation products of SOA, both of which produce an OA with a low O:C (0.1–0.6) (Aiken et al., 2008), which is likely to be phase separated from the inorganic aerosol. Second, to the best of our knowledge, AIOMFAC (Zuend et al., 2008, 2010; Zuend and Seinfeld, 2012) and the model of Topping et al. (2013) are currently the only modeling frameworks that can simultaneously solve for the thermodynamic state of a mixed organic-inorganic aerosol. While theoretically sophisticated, these models have not been evaluated against ambient measurements in box or 3D model applications. Further, AIOMFAC could potentially require many more tracers than are possible to accommodate in a 3D model, making it computationally expensive to implement. And finally, our current model simulations allow us to investigate changes in OA thermodynamics in response to water uptake, while maintaining an unchanged inorganic aerosol system.

For atmospheric aerosol, we anticipate that the activity coefficients for inorganic ions would be high enough to prevent them from partitioning into the organic phase. Given that some of the most polar constituents in OA could partition into the inorganic phase, the simulations performed in this work potentially offer an upper bound response of OA to water uptake by forcing all organics to be part of the same phase. The Non-polar POA simulation tests this upper bound response of the model to uncertainty in the miscibility of POA and SOA. The Chemically-resolved POA simulations test the upper bound response of the model to uncertainty in the miscibility of components of POA with SOA combined with the uncertainty in assuming an internal versus an external mixture. We expect that the response of OA to water uptake will be dampened if ambient aerosol were modeled as a single phase.

Table 2
List of simulations performed to assess the influence of water uptake on OA.

Description	POA hygroscopic?	POA surrogate	SOA hygroscopic?	Mixing state
Base	No		No	Internally mixed, POA mixes with SOA
Non-polar POA	No	All sources – C_{25} *n*-alkane	Yes	Internally mixed, POA does not mix with SOA
Chemically-resolved POA (internal)	Mobile sources – No Wood smoke – Yes Food cooking – Yes All other sources – Yes	Mobile sources – C_{25} *n*-alkane Wood smoke – Levoglucosan Food cooking – Monoglyceride All other sources – Octadecanoic acid	Yes	Internally mixed, polar POA mixes with SOA
Chemically-resolved POA (Source-oriented)	Mobile sources – No Wood smoke – Yes Food cooking – Yes All other sources – Yes	Mobile sources – C_{25} *n*-alkane Wood smoke – Levoglucosan Food cooking – Monoglyceride All other sources – Octadecanoic acid	Yes	Source-oriented mixture, polar POA mixes with SOA

3. Results

3.1. Base model

Model predictions of carbon monoxide (CO), daily-peak ozone (O_3) and nitrogen dioxide (NO_2) were compared to measurements made at ground sites monitored by the Environmental Protection Agency (EPA) and model predictions of elemental carbon (EC), OA, sulfate (SO_4^{2-}), nitrate (NO_3^-) and ammonium (NH_4^+) were compared to measurements made at the STN (Speciated Trends Network) and IMPROVE (Interagency Monitoring of Protected Visual Environments) air quality monitoring sites. We have excluded the model-measurement comparison of CO and NO_2 for the eastern US because the model predictions at 36 km × 36 km were too coarse to capture the measurements made at urban and semi-urban sites. The model-measurement comparison is presented using scatter plots in Figure S.1-2 and using statistical metrics in Table 3.

In SoCAB, model predictions of CO, O_3, EC, OA and nitrate for 2005 were mostly within a factor of two of measurements while sulfate and ammonium were, on average, under-predicted by a factor of two and NO_2, on average, was over-predicted by a factor of two. While NO_2 was over-predicted in 2005, predictions for most of the reactive nitrogen (NO, NO_2, HNO_3 and nitrate) compared favorably with measurements. More than 80% of the model-predicted sulfate came from the boundary conditions suggesting an absence of local sources. This implies that the sulfate under-prediction might be due to an under-estimation of SO_2 emissions. In the eastern US, EC, IMPROVE-OA and sulfate were predicted within a factor of two, while STN-OA was under-predicted. The model over-predicted peak O_3 concentrations, which might also explain over predictions of nitrate and, as a result, ammonium concentrations; higher O_3 at night translates to higher NO_2, N_2O_5 and HNO_3 production rates. According to model performance metrics suggested by Boylan and Russell (2006), the model performance was good to average for CO, NO_2, O_3, EC and OA and poor for sulfate, nitrate and ammonium in SoCAB. The model performance was good to average for O_3, EC, sulfate and ammonium and poor for OA and nitrate in the eastern US. Hence, one goal of the present study is to determine if the incorporation of organic-phase water in the calculations improves model performance for OA in the eastern US.

3.2. Water uptake and OA

3.2.1. Box model results

The interaction of OA and organic-phase water was first simulated in a box model to explore the general behavior. We studied two cases: system A only had non-volatile POA and system B only had semi-volatile and low-volatility SOA. In system A, we modeled POA either as a C_{25} *n*-alkane (nonhygroscopic and representative of diesel exhaust) or as levoglucosan (modestly hygroscopic and representative of biomass burning emissions). The molecular surrogates were chosen to represent the range of hygroscopicities observed for freshly emitted POA. In system B, the composition of the SOA model species was based on summer model predictions of CMAQ v4.7 in the southeast US (Pankow et al., 2015). The SOA in system B was composed of 1% alkane SOA, 12% aromatic SOA and 87% biogenic SOA by mass.

The results from the box model are presented in Fig. 1, where we plot the ratio of wet OA mass to dry OA mass (or OA enhancement) as a function of RH using colored bands. Here, the "wet" OA mass is the sum of OA and organic-phase water. The figure is analogous to particle growth curves expressed on a mass basis (Tang, 1976). Using dotted lines, we also plot the range of OA growth that would be predicted based on field measurements of OA hygroscopicity (κ = 0.03 to 0.22 for a 250 nm particle) (Jimenez et al., 2009). It should be noted that the model predictions expressed as OA enhancement might not be directly comparable to the κ values estimated from growth experiments. Mathematically, OA enhancement represents both the uptake of water and the partitioning of additional SOA mass while κ represents growth solely from the uptake of water. Experimentally, it is uncertain whether the κ estimated from growth measurements using a hygroscopic tandem differential mobility analyzer (HTDMA) would include shifts in gas/particle partitioning of SOA due to smaller residence times (Topping and McFiggans, 2012).

In system A, we found that there was no mass enhancement when the POA was assumed to be nonhygroscopic (C_{25} *n*-alkane) but some enhancement when the POA was moderately hygroscopic (levoglucosan); for example levoglucosan is predicted to absorb 36% of organic-phase water by mass at an RH of 80%. On average, this level of organic-phase water absorption was lower than that measured for ambient OA. The mass enhancement came about purely from the absorption of organic-phase water; POA was non-volatile and the organic-phase water did not change the POA mass. In system B, we found that there was substantial mass enhancement with increasing RH. In this system, the enhancement resulted not only from the absorption of organic-phase water but also from the change in the gas/particle partitioning of the SOA model species. We observed that the model universally shifted the partitioning of the SOA model species (except for the model species that represented sesquiterpene SOA) to the particle phase. At a C_{OA} of 5 μg m^{-3} and an RH between 60 and 80%, the absorption of organic-phase water accounted for 60% of the enhancement while the shift in gas/particle partitioning accounted for the remaining 40%. Further, we also observed that for the same RH, the

Table 3
Base model performance presented using four statistical metrics: predicted mean, observed mean, fractional bias and fractional error. Green, orange and yellow shading represent 'good', 'average' and 'poor' model performance (Boylan and Russell, 2006).

Domain	Network	Pollutant	Predicted Mean	Observed Mean	Fractional Bias (%)	Fractional Error (%)
SoCAB	EPA (ppb)	CO	395.6	371.2	13	43
		NO_2	36.2	18.5	58	66
		Peak O_3	83.9	65.1	27	33
	STN ($\mu g\ m^{-3}$)	EC	1.46	0.80	56	57
		OA	5.53	9.36	-54	54
		SO_4^{2-} (sulfate)	2.69	6.01	-74	74
		NO_3^- (nitrate)	3.01	5.11	-58	68
		NH_4^+ (ammonium)	1.67	3.49	-69	69
	IMPROVE ($\mu g\ m^{-3}$)	EC	0.56	0.65	-29	41
		OA	2.49	2.90	-28	42
		SO_4^{2-} (sulfate)	1.75	3.24	-57	59
		NO_3^- (nitrate)	1.25	1.43	-58	98
Eastern US	EPA (ppb)	Peak O_3	87.4	52.3	52	53
	STN ($\mu g\ m^{-3}$)	EC	0.67	0.64	8	48
		OA	2.84	6.38	-81	90
		SO_4^{2-} (sulfate)	7.79	5.38	43	61
		NO_3^- (nitrate)	1.31	0.64	36	89
		NH_4^+ (ammonium)	3.07	1.84	56	68
	IMPROVE ($\mu g\ m^{-3}$)	EC	0.49	0.53	-6	43
		OA	2.40	2.49	-11	54
		SO_4^{2-} (sulfate)	7.10	4.92	46	66
		NO_3^- (nitrate)	1.38	0.39	68	115

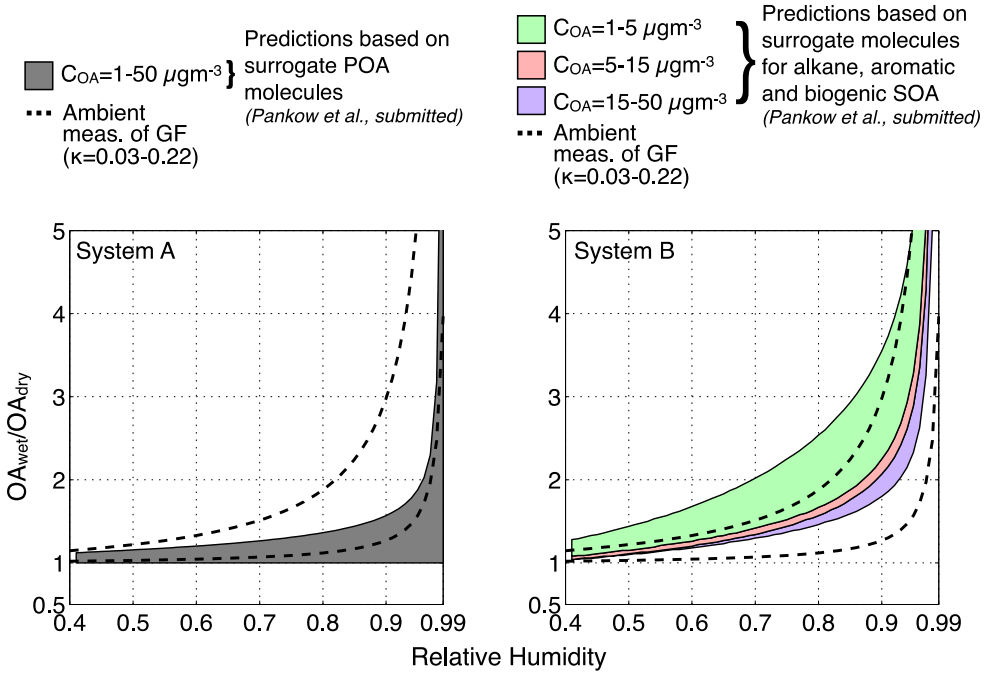

Fig. 1. The general behavior of the box model is captured by plotting the OA enhancement or OA mass growth (OA_{wet}/OA_{dry})as a function of relative humidity; the different bands represent OA concentration ranges. OA_{wet} includes both OA and organic-phase water. System A represents POA-only OA and system B represents a semi-volatile SOA only OA. OA enhancement based on ambient measurements of κ is shown using the dotted lines.

enhancement was larger for lower OA concentrations. For example, at an RH of 80%, the mass enhancement was 150% at 1 $\mu g\ m^{-3}$ in contrast to 60% at 15 $\mu g\ m^{-3}$. The theoretical explanation for this observation was provided by Pankow (1994): at lower OA concentrations more semi-volatile vapors are available to condense than are available at higher OA concentrations. For system B, on

average, the mass enhancement with RH was higher than that measured for ambient OA. Overall, the box model suggests that non-volatile OA results in much smaller mass enhancements from the uptake of water but semi-volatile OA allows for much larger mass enhancements from both the uptake of water and shifts in gas/particle partitioning. It is likely that in a system with both POA and SOA, the mass enhancement would lie somewhere between the results predicted by system A and system B and potentially agree well with the ambient measurements of enhancement as a function of RH.

3.2.2. 3D model results

Concentrations of SOA and organic-phase water from all simulations are plotted in Fig. 2 for SoCAB and in Fig. 3 for the eastern US. For the Base simulation, SOA concentrations were lower in SoCAB (1 μg m^{-3}) but much higher in the eastern US (>1.5 μg m^{-3}) over most of the domain and >4 μg m^{-3} in the southeastern US. In contrast, POA concentrations were higher in the SoCAB (~5–7 μg m^{-3} in the urban areas and ~1–2 μg m^{-3} elsewhere) and lower in the eastern US (~2–3 μg m^{-3} in the urban areas and 0.5–1 μg m^{-3} elsewhere); POA concentrations for both domains are plotted in Figure S.3. The SOA in SoCAB, in a representative urban location, was about 25% anthropogenic and 75% biogenic; the SOA in the eastern US was almost all biogenic (>90%). In SoCAB, SOA concentrations remained about the same between all the simulations suggesting that organic-phase water did very little to change the gas/particle partitioning of the SOA model species. In contrast, the absorption of organic-phase water altered the gas/particle partitioning of SOA and increased SOA concentrations in the eastern US substantially. The enhancement was most pronounced in the southeast US where SOA concentrations increased, on average, by 50–100% for the Non-polar POA and Chemically-resolved POA (source-oriented) simulations and 150% for the Chemically-resolved POA (internal) simulations. The amount of organic-phase water was about 0.1–0.2 μg m^{-3} in SoCAB and about 2–4 μg m^{-3} in the Southeast US. With very small enhancements in SOA mass concentrations, the inclusion of organic-phase water did not change OA model performance in the SoCAB; we should note that the Base model already offers 'good' and 'average' model performance for OA in SoCAB (see Table 3). With larger enhancements in SOA mass concentrations and larger uptake of water, the model performance was marginally improved in the eastern US (see Table 4 for statistical metrics); the fractional bias and fractional error were slightly lower for the simulations that included organic-phase water. Here, only POA and SOA was summed to determine model-predicted OA mass concentrations since measurements of OA (or to be precise, organic carbon) at STN and IMPROVE sites are dry measurements and do not include water.

In Fig. 4, we plot daily-averaged concentrations of SOA and organic-phase water, temperature and RH in one city within each of the two domains for a period of two weeks: central Los Angeles, CA in SoCAB (panels a, b and c) and Atlanta, GA in the eastern US (panels c, d and e). In central Los Angeles, we found that the SOA concentrations did not change significantly across the four simulations, consistent with the results for SoCAB. The water uptake by SOA in the Non-polar POA simulation and by POA + SOA in the Chemically-resolved POA (internal/source-oriented) simulations was the same (2-week average of 0.2 μg m^{-3}). In contrast, water uptake caused modest enhancement in SOA concentrations for the Non-polar POA (75%, averaged over a 2-week period), Chemically-resolved POA (internal) (130% averaged over a 2-week period) and Chemically-resolved POA (source-oriented) (81%, averaged

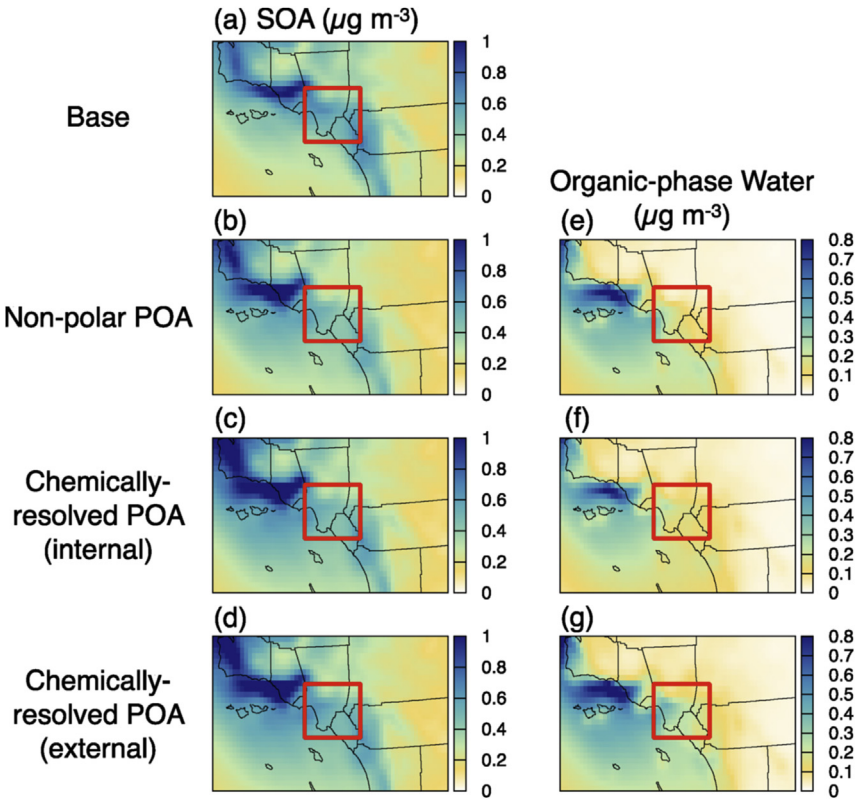

Fig. 2. 2-week averaged concentrations of SOA (a–d) and organic-phase water (e–g) for SoCAB for the Base, Non-polar POA, Chemically-resolved POA (internal) and Chemically-resolved POA (source-oriented) simulations. Urban area marked with a red box.

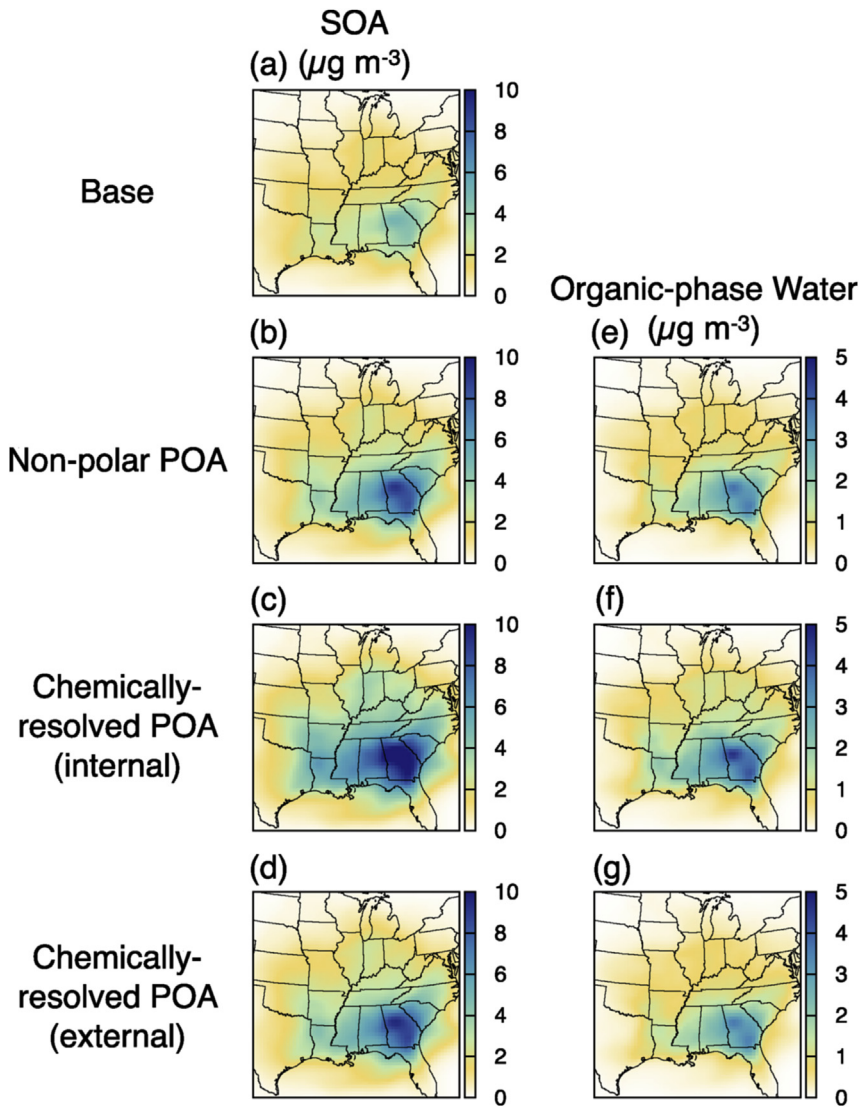

Fig. 3. 2-week averaged concentrations of SOA (a–d) and Organic-phase water (e–g) for the eastern US for the Base, Non-polar POA, Chemically-resolved POA (internal) and Chemically-resolved POA (source-oriented) simulations.

Table 4
Model performance for the four simulations performed over the eastern US presented using four statistical metrics: predicted mean, observed mean, fractional bias and fractional error. Green, orange and yellow shading represent 'good', 'average' and 'poor' model performance (Boylan and Russell, 2006).

Domain	Simulation	Network	Predicted Mean (μg m^{-3})	Observed Mean (μg m^{-3})	Fractional Bias (%)	Fractional Error (%)
Eastern US	Base	STN	2.84	6.38	-81	90
		IMPROVE	2.40	2.49	-11	54
	Non-polar POA	STN	3.28	6.38	-73	86
		IMPROVE	3.05	2.49	3	62
	Chemically-resolved POA (internal)	STN	4.18	6.38	-57	78
		IMPROVE	3.97	2.49	21	69
	Chemically-resolved POA (source-oriented)	STN	3.29	6.38	-73	86
		IMPROVE	3.10	2.49	4	62

over a 2-week period) simulations in Atlanta. It should be noted that the temperatures were similar but the RH was higher in Atlanta (>0.8) than in Los Angeles (<0.8) over that two-week period. The differences in SOA concentrations between the Non-

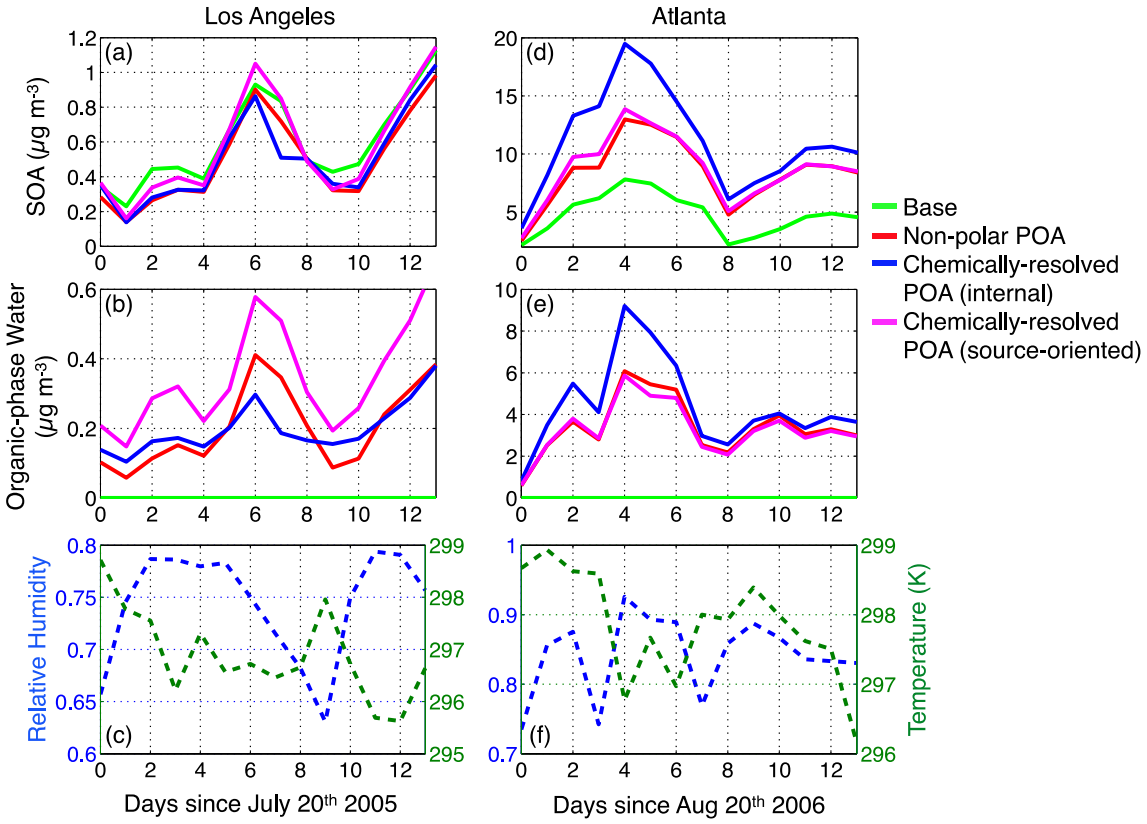

Fig. 4. Predicted daily-averaged concentrations of SOA and organic-phase water in μg m^{-3} in (a–b) central Los Angeles and (c–d) Atlanta for three different simulations.

polar POA and Chemically-resolved POA (internal) simulations can be explained by the assumptions made about POA and SOA miscibility. In the Non-polar POA simulation only SOA absorbed organic-phase water (2-week average of 3.4 μg m^{-3}) while in the Chemically-resolved POA (internal) simulations both the polar parts of POA and SOA absorbed organic-phase water (2-week average of 4.4 μg m^{-3}). In the Chemically-resolved POA (internal) simulations, both the additional organic-phase water and POA contributed to further shifting the gas/particle partitioning of SOA to the particle-phase. The combined effect was to increase SOA concentrations even further. The predictions from the Chemically-resolved (source-oriented) simulations were different from the Chemically-resolved POA (internal) simulations suggesting that assumptions about mixing have an effect on SOA concentrations. The predictions from the Chemically-resolved (source-oriented) simulations were most similar to predictions from the Non-polar POA simulation (see Figure S.4). Based on the results of the box model (Section 3.2.1), the mass enhancements in the eastern US (and Atlanta) are stronger because the OA is dominated by semi-volatile SOA while the mass enhancements in the SoCAB (and Los Angeles) are weaker as a result of a non-volatile POA dominated OA.

In Fig. 5, we plot the 2-week averaged diurnal concentrations for total OA (POA + SOA + organic-phase water) and RH. The diurnal trend in the total OA concentration for the Base simulation, at both central Los Angeles and Atlanta, can be explained as follows. The increase in OA between 5 and 10 am can be attributed to the "morning traffic rush hour" and the decrease after that can be attributed to dilution/mixing into an increasing boundary layer. The increase in OA between 4 and 7 pm can be attributed to an "evening traffic rush hour" and the subsequent increase after 7 pm can be attributed to the collapse of the boundary layer where emissions/production of OA are limited to the surface layer. In central Los Angeles, the POA-dominated OA in the Non-polar and Chemically-resolved POA simulations did not respond to the diurnal change in RH. In Atlanta, the SOA-dominated OA in the Non-polar and Chemically-resolved POA simulations was a factor of 2–3 higher than the Base simulation when the RH was high (midnight to noon) and a factor of 1.5–2 higher than the Base simulation when the RH was low (mid-afternoon).

The 2-week averaged concentration of POA + SOA + organic-phase water for the different simulations is plotted in Fig. 6. The SOA is split into its contribution from anthropogenic and biogenic sources. As explained earlier, in central Los Angeles the SOA concentration in all 3 simulations remained the same while the organic-phase water concentration changed based on whether only SOA or both polar POA and SOA were involved in water uptake. As seen earlier, in Atlanta the SOA concentrations increased in the Non-polar and Chemically-resolved POA simulations and almost all of the increase appeared to come from increases in biogenic SOA. The organic-phase water concentration in Atlanta between the Non-polar and Chemically-resolved POA simulations was quite similar.

Fig. 7 has the same format as Fig. 1 but the displayed data points are obtained from the surface layer of the full 3D air quality model as opposed to the simple box model. Here, daily-averaged OA enhancement (defined as the ratio of the OA concentration in the Non-polar or Chemically-resolved POA simulations to the OA concentration in the Base simulation) is plotted as a function of RH at all grid cells in the domain over a period of 2 weeks to determine whether the model predictions at central Los Angeles and Atlanta were representative of their domain. To avoid visual clutter, we only plot 4% of the ~19,000 points in SoCAB and the ~42,000 points in the eastern US. SoCAB was dominated by POA and hence box model predictions from system A (only POA) are presented with the

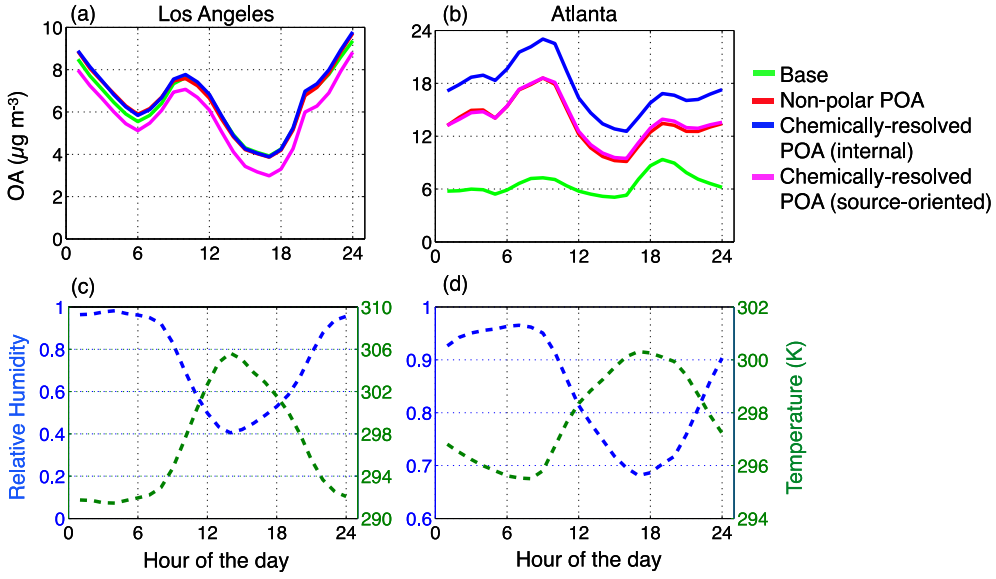

Fig. 5. Predicted 2-week averaged diurnal concentrations of total OA (POA + SOA + Organic-phase water) in μg m^{-3}, temperature in K and relative humidity in (a,c) central Los Angeles and (b,d) Atlanta for four different simulations.

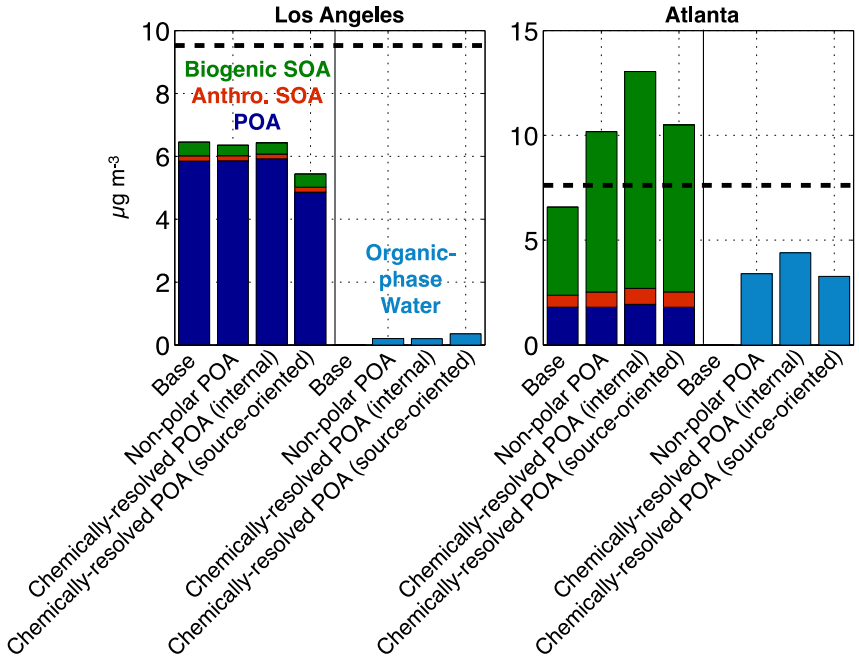

Fig. 6. Predicted 2-week averaged values of SOA and Organic-phase water in μg m^{-3} for (a) central Los Angeles and (b) Atlanta. SOA is split by source: biogenic and anthropogenic.

SoCAB results. The eastern US was dominated by SOA and hence box model predictions from system B (only SOA) are presented with the eastern US results. We found that the OA in SoCAB behaved like system A (only POA) and there was very little enhancement in total OA concentrations with RH and very little water uptake; for example we predict an average total OA enhancement of 10% at an RH of 80%. The OA appeared to behave like a particle with a κ less than 0.03, with very little growth even at high RH. In sharp contrast, the eastern US behaved like a mix of systems A (only POA) and B (only SOA) and had substantial enhancement in total OA concentrations with RH. At an RH of 80%, we predicted an average total OA enhancement of 60% for the Non-polar POA simulation, 102% for the Chemically-resolved POA (internal) simulation and 63% for the Chemically-resolved (source-oriented) simulation. The OA appears to behave like a particle with a κ between 0.1 and 0.2.

4. Summary and discussion

In this work, we explicitly modeled the water uptake by OA and used an iterative gas/particle partitioning model with the UNIFAC activity model to calculate the subsequent effect on SOA. Regional calculations were performed with a chemical transport model (UCD/CIT source-oriented model) to make air quality predictions in SoCAB and the eastern US. Water uptake by OA can influence gas/particle partitioning of SOA but the magnitude of its effect differed strongly with location. In California, drier conditions (lower

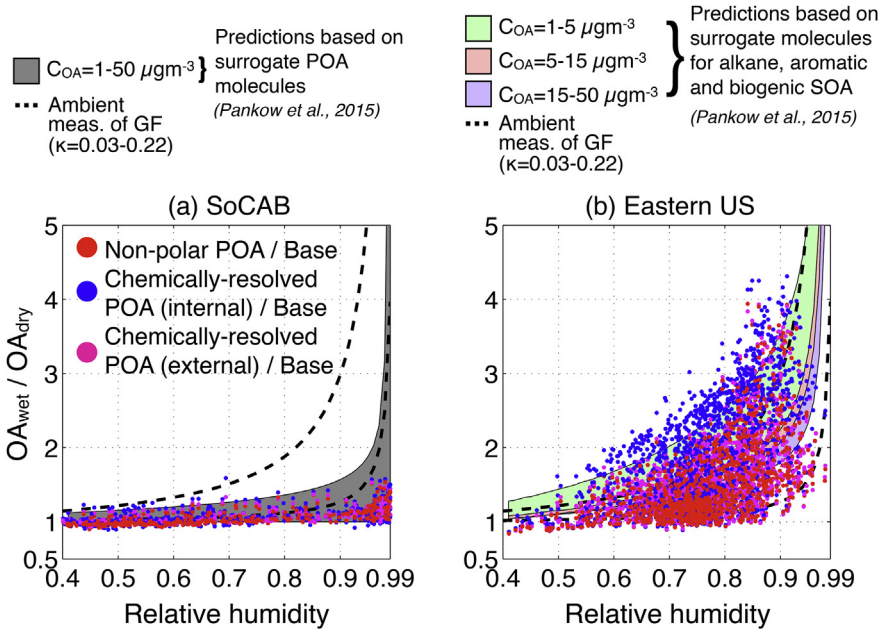

Fig. 7. Predicted daily-averaged OA enhancement (or OA mass growth) plotted as a function of relative humidity for two different simulations across the whole modeled domain (dots); panel (a) is for SoCAB and panel (b) is for the eastern US. Enhancement is calculated as the ratio of OA predicted by the simulation to the OA predicted by the BASE simulation. Each dot represents enhancement at a particular grid cell on a particular day. Box model predictions of a POA-dominant (a) and SOA-dominant system are presented in the background. Dotted lines show OA enhancement based on κ values estimated for ambient OA.

humidity) and the dominance of non-volatile POA over SOA meant that very little organic-phase water was absorbed by OA (<0.2 μg m^{-3}) and the organic-phase water had a small effect on the gas/particle partitioning of SOA. In the eastern US, a significant amount of organic-phase water was absorbed by OA (maximum of 5 μg m^{-3}) leading to changes in SOA gas/particle partitioning. On average, total OA mass concentrations increased by approximately 20% for every 10% increase in RH above 40%. Simulations over the eastern US also suggested that the mixing state of OA (internally versus source-oriented externally mixed) had a modest effect on total OA concentrations when accounting for the influence of water uptake; internally mixed simulations predicted 30% higher concentrations of OA than source-oriented externally mixed simulations. In summary, this work indicates that water uptake can significantly affect predicted OA mass concentrations in areas with high humidity and significant SOA formation. Chemical transport models should include organic-phase water in regions where these conditions exist. Atmospheric aerosol contains mixed phases with both organic and inorganic constituents. By assuming phase separation of the organic and inorganic components, the present study simulates an upper bound response of the influence of water uptake on OA. Future work should model the thermodynamics (e.g., gas/particle partitioning, phase separation) of all aerosol components simultaneously using more comprehensive models like AIOMFAC (Zuend and Seinfeld, 2012) and those based on the work of Topping et al. (2013). Further, there is uncertainty about the miscibility amongst various constituents of OA and the mixing state of urban aerosol that could control the influence of water uptake on OA. While important, this work hints that the uncertainty in miscibility and mixing state has a small (in SoCAB) to modest (in the eastern US) impact on model predictions of OA. Regardless, future work should be mindful of these uncertainties that are commonly discounted in large-scale models.

Acknowledgments

This work was funded by the California Air Resources Board under contract #11-755. The statements and conclusions in this report are those of the authors and not necessarily those of the California Air Resources Board. The mention of commercial products, their source, or their use in connection with material reported herein is not to be construed as actual or implied endorsement of such products.

Appendix A. Supplementary data

Supplementary data related to this article can be found at http://dx.doi.org/10.1016/j.atmosenv.2016.01.001.

References

Aiken, A.C., DeCarlo, P.F., Kroll, J.H., Worsnop, D.R., Huffman, J.A., Docherty, K.S., Ulbrich, I.M., Mohr, C., Kimmel, J.R., Sueper, D., et al., 2008. O/C and OM/OC ratios of primary, secondary, and ambient organic aerosols with high-resolution time-of-flight aerosol mass spectrometry. Environ. Sci. Technol. 42, 4478–4485.
Ansari, A.S., Pandis, S.N., 2000. Water absorption by secondary organic aerosol and its effect on inorganic aerosol behavior. Environ. Sci. Technol. 34, 71–77.
Asa-Awuku, A., Miracolo, M., Kroll, J., Robinson, A., Donahue, N., 2009. Mixing and phase partitioning of primary and secondary organic aerosols. Geophys. Res. Lett. 36, L15827. http://dx.doi.org/10.1029/2009GL039301.
Baker, K.R., Misenis, C., Obland, M.D., Ferrare, R.A., Scarino, A.J., Kelly, J.T., 2013. Evaluation of surface and upper air fine scale WRF meteorological modeling of the May and June 2010 CalNex period in California. Atmos. Environ. 80, 299–309.
Barley, M., Topping, D., Jenkin, M., McFiggans, G., 2009. Sensitivities of the absorptive partitioning model of secondary organic aerosol formation to the inclusion of water. Atmos. Chem. Phys. 9, 2919–2932.
Bertram, A.K., Martin, S.T., Hanna, S.J., Smith, M.L., Bodsworth, A., Chen, Q., Kuwata, M., Liu, A., You, Y., Zorn, S.R., 2011. Predicting the relative humidities of liquid-liquid phase separation, efflorescence, and deliquescence of mixed particles of ammonium sulfate, organic material, and water using the organic-to-sulfate mass ratio of the particle and the oxygen-to-carbon elemental ratio of the organic component. Atmos. Chem. Phys. 11, 10995–11006.
Bowman, F.M., Karamalegos, A.M., 2002. Estimated effects of composition on secondary organic aerosol mass concentrations. Environ. Sci. Technol. 36, 2701–2707.

Boylan, J.W., Russell, A.G., 2006. PM and light extinction model performance metrics, goals, and criteria for three-dimensional air quality models. Atmos. Environ. 40, 4946–4959.
CARB, 2011. EMFAC (Mobile Source Emission Inventory). In: EMFAC (Mobile Source Emission Inventory). California Air Resources Board.
Carlton, A.G., Bhave, P.V., Napelenok, S.L., Edney, E.O., Sarwar, G., Pinder, R.W., Pouliot, G.A., Houyoux, M., 2010. Model representation of secondary organic aerosol in CMAQv4. 7. Environ. Sci. Technol. 44, 8553–8560.
Carter, W.P., Heo, G., 2013. Development of revised SAPRC aromatics mechanisms. Atmos. Environ. 77, 404–414.
Chang, E.I., Pankow, J.F., 2010. Organic particulate matter formation at varying relative humidity using surrogate secondary and primary organic compounds with activity corrections in the condensed phase obtained using a method based on the Wilson equation. Atmos. Chem. Phys. 10, 5475–5490.
Clegg, S.L., Seinfeld, J.H., Brimblecombe, P., 2001. Thermodynamic modelling of aqueous aerosols containing electrolytes and dissolved organic compounds. J. Aerosol Sci. 32, 713–738.
Davis, J.M., Bhave, P.V., Foley, K.M., 2008. Parameterization of N2O5 reaction probabilities on the surface of particles containing ammonium, sulfate, and nitrate. Atmos. Chem. Phys. 8, 5295–5311.
Emmons, L.K., Walters, S., Hess, P.G., Lamarque, J.F., Pfister, G.G., Fillmore, D., Granier, C., Guenther, A., Kinnison, D., Laepple, T., Orlando, J., Tie, X., Tyndall, G., Wiedinmyer, C., Baughcum, S.L., Kloster, S., 2010. Description and evaluation of the Model for Ozone and Related chemical Tracers, version 4 (MOZART-4). Geosci. Model Dev. 3, 43–67. http://dx.doi.org/10.5194/gmd-3-43-2010.
Fredenslund, A., Jones, R.L., Prausnitz, J.M., 1975. Group-contribution estimation of activity coefficients in nonideal liquid mixtures. AIChE J. 21, 1086–1099.
Goldstein, A.H., Galbally, I.E., 2007. Known and unexplored organic constituents in the earth's atmosphere. Environ. Sci. Technol. 41, 1514–1521. http://dx.doi.org/10.1021/es072476p.
Griffin, R.J., Dabdub, D., Seinfeld, J.H., 2005. Development and initial evaluation of a dynamic species-resolved model for gas phase chemistry and size-resolved gas/particle partitioning associated with secondary organic aerosol formation. J. Geophys. Res. 110.
Guenther, A., Karl, T., Harley, P., Wiedinmyer, C., Palmer, P., Geron, C., 2006. Estimates of global terrestrial isoprene emissions using MEGAN (Model of emissions of gases and aerosols from Nature). Atmos. Chem. Phys. 6, 3181–3210.
Hallquist, M., Wenger, J.C., Baltensperger, U., Rudich, Y., Simpson, D., Claeys, M., Dommen, J., Donahue, N.M., George, C., Goldstein, A.H., Hamilton, J.F., Herrmann, H., Hoffmann, T., Iinuma, Y., Jang, M., Jenkin, M.E., Jimenez, J.L., Kiendler-Scharr, A., Maenhaut, W., McFiggans, G., Mentel, T.F., Monod, A., Prévôt, A.S.H., Seinfeld, J.H., Surratt, J.D., Szmigielski, R., Wildt, J., 2009. The formation, properties and impact of secondary organic aerosol: current and emerging issues. Atmos. Chem. Phys. 9, 5155–5236. http://dx.doi.org/10.5194/acp-9-5155-2009.
Hu, J., Ying, Q., Chen, J., Mahmud, A., Zhao, Z., Chen, S.-H., Kleeman, M.J., 2010. Particulate air quality model predictions using prognostic vs. diagnostic meteorology in central California. Atmos. Environ. 44, 215–226.
Hu, J., Howard, C.J., Mitloehner, F., Green, P.G., Kleeman, M.J., 2012. Mobile source and livestock feed contributions to regional ozone formation in Central California. Environ. Sci. Technol. 46, 2781–2789.
GBD Heatmap, 2013. http://vizhub.healthdata.org/irank/heat.php. access: 9/2014.
Jimenez, J.L., Canagaratna, M.R., Donahue, N.M., Prevot, A.S.H., Zhang, Q., Kroll, J.H., DeCarlo, P.F., Allan, J.D., Coe, H., Ng, N.L., Aiken, A.C., Docherty, K.S., Ulbrich, I.M., Grieshop, A.P., Robinson, A.L., Duplissy, J., Smith, J.D., Wilson, K.R., Lanz, V.A., Hueglin, C., Sun, Y.L., Tian, J., Laaksonen, A., Raatikainen, T., Rautiainen, J., Vaattovaara, P., Ehn, M., Kulmala, M., Tomlinson, J.M., Collins, D.R., Cubison, M.J.E., Dunlea, J., Huffman, J.A., Onasch, T.B., Alfarra, M.R., Williams, P.I., Bower, K., Kondo, Y., Schneider, J., Drewnick, F., Borrmann, S., Weimer, S., Demerjian, K., Salcedo, D., Cottrell, L., Griffin, R., Takami, A., Miyoshi, T., Hatakeyama, S., Shimono, A., Sun, J.Y., Zhang, Y.M., Dzepina, K., Kimmel, J.R., Sueper, D., Jayne, J.T., Herndon, S.C., Trimborn, A.M., Williams, L.R., Wood, E.C., Middlebrook, A.M., Kolb, C.E., Baltensperger, U., Worsnop, D.R., 2009. Evolution of organic aerosols in the atmosphere. Science 326, 1525–1529. http://dx.doi.org/10.1126/science.1180353.
Kanakidou, M., Seinfeld, J.H., Pandis, S.N., Barnes, I., Dentener, F.J., Facchini, M.C., Van Dingenen, R., Ervens, B., Nenes, A., Nielsen, C.J., Swietlicki, E., Putaud, J.P., Balkanski, Y., Fuzzi, S., Horth, J., Moortgat, G.K., Winterhalter, R., Myhre, C.E.L., Tsigaridis, K., Vignati, E., Stephanou, E.G., Wilson, J., 2005. Organic aerosol and global climate modelling: a review. Atmos. Chem. Phys. 5, 1053–1123. http://dx.doi.org/10.5194/acp-5-1053-2005.
Kleeman, M.J., Cass, G.R., Eldering, A., 1997. Modeling the airborne particle complex as a source-oriented external mixture. J. Geophys. Res. Atmos. 102, 21355–21372.
Kleeman, M.J., Cass, G.R., 2001. A 3D eulerian source-oriented model for an externally mixed aerosol. Environ. Sci. Technol. 35, 4834–4848.
Koehler, K.A., Kreidenweis, S.M., DeMott, P.J., Petters, M.D., Prenni, A.J., Carrico, C.M., 2009. Hygroscopicity and cloud droplet activation of mineral dust aerosol. Geophys. Res. Lett. 36.
LeMone, M.A., Chen, F., Tewari, M., Dudhia, J., Geerts, B., Miao, Q., Coulter, R.L., Grossman, R.L., 2010a. Simulating the IHOP_2002 fair-weather CBL with the WRF-ARW-Noah modeling system. Part II: structures from a few kilometers to 100 km across. Mon. Weather Rev. 138, 745–764.
LeMone, M.A., Chen, F., Tewari, M., Dudhia, J., Geerts, B., Miao, Q., Coulter, R.L., Grossman, R.L., 2010b. Simulating the IHOP_2002 fair-weather CBL with the WRF-ARW-Noah modeling system. Part I: surface fluxes and CBL structure and evolution along the eastern track. Mon. Weather Rev. 138, 722–744.
Liu, X., Wang, J., 2010. How important is organic aerosol hygroscopicity to aerosol indirect forcing? Environ. Res. Lett. 5, 044010.
Mahmud, A., Hixson, M., Hu, J., Zhao, Z., Chen, S.-H., Kleeman, M., 2010. Climate impact on airborne particulate matter concentrations in California using seven year analysis periods. Atmos. Chem. Phys. 10, 11097–11114.
Ming, Y., Russell, L.M., 2002. Thermodynamic equilibrium of organic-electrolyte mixtures in aerosol particles. AIChE J. 48, 1331–1348.
Nenes, A., Pandis, S.N., Pilinis, C., 1998. ISORROPIA: a new thermodynamic equilibrium model for multiphase multicomponent inorganic aerosols. Aquat. Geochem. 4, 123–152.
Pachauri, R.K., Allen, M.R., Barros, V.R., Broome, J., Cramer, W., Christ, R., Church, J.A., Clarke, L., Dahe, Q., Dasgupta, P., Dubash, N.K., Edenhofer, O., Elgizouli, I., Field, C.B., Forster, P., Friedlingstein, P., Fuglestvedt, J., Gomez-Echeverri, L., Hallegatte, S., Hegerl, G., Howden, M., Jiang, K., Jimenez Cisneroz, B., Kattsov, V., Lee, H., Mach, K.J., Marotzke, J., Mastrandrea, M.D., Meyer, L., Minx, J., Mulugetta, Y., O'Brien, K., Oppenheimer, M., Pereira, J.J., Pichs-Madruga, R., Plattner, G.K., Pörtner, H.-O., Power, S.B., Preston, B., Ravindranath, N.H., Reisinger, A., Riahi, K., Rusticucci, M., Scholes, R., Seyboth, K., Sokona, Y., Stavins, R., Stocker, T.F., Tschakert, P., van Vuuren, D., van Ypserle, J.P., 2014. Climate change 2014. In: Pachauri, R.K., Meyer, L. (Eds.), Synthesis Report. Contribution of Working Groups I, II and III to the Fifth Assessment Report of the Intergovernmental Panel on Climate Change. IPCC, Geneva, Switzerland, p. 151.
Pankow, J.F., 1994. An absorption model of gas/particle partitioning of organic compounds in the atmosphere. Atmos. Environ. 28, 185–188.
Pankow, J.F., Asher, W.E., 2008. SIMPOL. 1: a simple group contribution method for predicting vapor pressures and enthalpies of vaporization of multifunctional organic compounds. Atmos. Chem. Phys. 8, 2773–2796.
Pankow, J.F., Chang, E.I., 2008. Variation in the sensitivity of predicted levels of atmospheric organic particulate matter (OPM). Environ. Sci. Technol. 42, 7321–7329.
Pankow, J.F., Marks, M.C., Barsanti, K.C., Mahmud, A., Asher, W.E., Li, J., Ying, Q., Jathar, S.H., Kleeman, M.J., 2015. Molecular view modeling of atmospheric organic particulate matter incorporating molecular structure and co-condensation of water. Atmos. Environ. 122, 400–408.
Peng, C., Chan, M.N., Chan, C.K., 2001. The hygroscopic properties of dicarboxylic and multifunctional acids: measurements and UNIFAC predictions. Environ. Sci. Technol. 35, 4495–4501.
Petters, M., Kreidenweis, S., 2007. A single parameter representation of hygroscopic growth and cloud condensation nucleus activity. Atmos. Chem. Phys. 7, 1961–1971.
Pringle, K.J., Tost, H., Pozzer, A., Pöschl, U., Lelieveld, J., 2010. Global distribution of the effective aerosol hygroscopicity parameter for CCN activation. Atmos. Chem. Phys. 10, 5241–5255.
Pun, B.K., 2008. Development and initial application of the sesquiversion of MADRID. J. Geophys. Res. 113 http://dx.doi.org/10.1029/2008JD009888. D12212.
Schwarz, J.P., Gao, R.S., Spackman, J.R., Watts, L.A., Thomson, D.S., Fahey, D.W., Ryerson, T.B., Peischl, J., Holloway, J.S., Trainer, M., Frost, G.J., Baynard, T., Lack, D.A., de Gouw, J.A., Warneke, C., Del Negro, L., 2008. A.: measurement of the mixing state, mass, and optical size of individual black carbon particles in urban and biomass burning emissions. Geophys. Res. Lett. 35 http://dx.doi.org/10.1029/2008GL033968.
Seinfeld, J.H., Erdakos, G.B., Asher, W.E., Pankow, J.F., 2001. Modeling the formation of secondary organic aerosol (SOA). 2. The predicted effects of relative humidity on aerosol formation in the α-pinene-, β-pinene-, sabinene-, Δ^3-carene-, and cyclohexene-ozone systems. Environ. Sci. Technol. 35, 1806–1817.
Smith, M.L., You, Y., Kuwata, M., Bertram, A.K., Martin, S.T., 2013. Phase transitions and phase miscibility of mixed particles of ammonium sulfate, toluene-derived secondary organic material, and water. J. Phys. Chem. A 117, 8895–8906.
Song, C., Zaveri, R., Alexander, M., Thornton, J., Madronich, S., Ortega, J., Zelenyuk, A., Yu, X., Laskin, A., Maughan, D., 2007. Effect of hydrophobic primary organic aerosols on secondary organic aerosol formation from ozonolysis of a-pinene. Geophys. Res. Lett. 34.
Song, C., Zaveri, R.A., Shilling, J.E., Alexander, M.L., Newburn, M., 2011. Effect of hydrophilic organic seed aerosols on secondary organic aerosol formation from ozonolysis of alpha-pinene. Environ. Sci. Technol. 45, 7323–7329. http://dx.doi.org/10.1021/es201225c.
Tang, I.N., 1976. Phase transformation and growth of aerosol particles composed of mixed salts. J. Aerosol Sci. 7, 361–371.
Topping, D., Barley, M., McFiggans, G., 2013. Including phase separation in a unified model to calculate partitioning of vapours to mixed inorganic–organic aerosol particles. Faraday Discuss. 165, 273–288.
Topping, D.O., McFiggans, G., 2012. Tight coupling of particle size, number and composition in atmospheric cloud droplet activation. Atmos. Chem. Phys. 12, 3253–3260.
Tsigaridis, K., Daskalakis, N., Kanakidou, M., Adams, P.J., Artaxo, P., Bahadur, R., Balkanski, Y., Bauer, S.E., Bellouin, N., Benedetti, A., Bergman, T., Berntsen, T.K., Beukes, J.P., Bian, H., Carslaw, K.S., Chin, M., Curci, G., Diehl, T., Easter, R.C., Ghan, S.J., Gong, S.L., Hodzic, A., Hoyle, C.R., Iversen, T., Jathar, S., Jimenez, J.L., Kaiser, J.W., Kirkevåg, A., Koch, D., Kokkola, H., Lee, Y.H., Lin, G., Liu, X., Luo, G., Ma, X., Mann, G.W., Mihalopoulos, N., Morcrette, J.J., Müller, J.F., Myhre, G., Myriokefalitakis, S., Ng, N.L., O'Donnell, D., Penner, J.E., Pozzoli, L., Pringle, K.J., Russell, L.M., Schulz, M., Sciare, J., Seland, Ø., Shindell, D.T., Sillman, S.,

Skeie, R.B., Spracklen, D., Stavrakou, T., Steenrod, S.D., Takemura, T., Tiitta, P., Tilmes, S., Tost, H., van Noije, T., van Zyl, P.G., von Salzen, K., Yu, F., Wang, Z., Wang, Z., Zaveri, R.A., Zhang, H., Zhang, K., Zhang, Q., Zhang, X., 2014. The AeroCom evaluation and intercomparison of organic aerosol in global models. Atmos. Chem. Phys. 14, 10845–10895. http://dx.doi.org/10.5194/acp-14-10845-2014.

Weingartner, E., Burtscher, H., Baltensperger, U., 1997. Hygroscopic properties of carbon and diesel soot particles. Atmos. Environ. 31, 2311–2327.

Wiedinmyer, C., Akagi, S., Yokelson, R.J., Emmons, L., Al-Saadi, J., Orlando, J., Soja, A., 2011. The fire INventory from NCAR (FINN): a high resolution global model to estimate the emissions from open burning. Geosci. Model Dev. 4, 625.

Yatavelli, R.L.N., Lopez-Hilfiker, F., Wargo, J.D., Kimmel, J.R., Cubison, M.J., Bertram, T.H., Jimenez, J.L., Gonin, M., Worsnop, D.R., Thornton, J.A., 2012. A chemical ionization high-resolution time-of-flight mass spectrometer coupled to a micro orifice volatilization impactor (MOVI-HRToF-CIMS) for analysis of gas and particle-phase organic species. Aerosol Sci. Technol. 46, 1313–1327.

You, Y., Renbaum-Wolff, L., Bertram, A.K., 2013. Liquid–liquid phase separation in particles containing organics mixed with ammonium sulfate, ammonium bisulfate, ammonium nitrate or sodium chloride. Atmos. Chem. Phys. 13, 11723–11734.

You, Y., Smith, M.L., Song, M., Martin, S.T., Bertram, A.K., 2014. Liquid–liquid phase separation in atmospherically relevant particles consisting of organic species and inorganic salts. Int. Rev. Phys. Chem. 33, 43–77.

Zuend, A., Marcolli, C., Luo, B.P., Peter, T., 2008. A thermodynamic model of mixed organic-inorganic aerosols to predict activity coefficients. Atmos. Chem. Phys. 8, 4559–4593.

Zuend, A., Marcolli, C., Peter, T., Seinfeld, J.H., 2010. Computation of liquid-liquid equilibria and phase stabilities: implications for RH-dependent gas/particle partitioning of organic-inorganic aerosols. Atmos. Chem. Phys. 10, 7795–7820.

Zuend, A., Seinfeld, J.H., 2012. Modeling the gas-particle partitioning of secondary organic aerosol: the importance of liquid-liquid phase separation. Atmos. Chem. Phys. 12, 3857–3882.